

Published in final edited form as:

J Alzheimers Dis. 2013 ; 35(4): 751–760. doi:10.3233/JAD-130080.

Altered Default Mode Network Connectivity in Older Adults with Cognitive Complaints and Amnesic Mild Cognitive Impairment

Yang Wang^a, Shannon L. Risacher^a, John D. West^a, Brenna C. McDonald^{a,b}, Tamiko R. MaGee^a, Martin R. Farlow^b, Sujuan Gao^c, Darren P. O'Neill^a, and Andrew J. Saykin^{a,*}

^aCenter for Neuroimaging, Department of Radiology and Imaging Sciences, Indiana University School of Medicine, Indianapolis, IN, USA

^bDepartment of Neurology, Indiana University School of Medicine, Indianapolis, IN, USA

^cDepartment of Biostatistics, Indiana University School of Medicine, Indianapolis, IN, USA

Abstract

Default mode network (DMN) disruption has been reported in Alzheimer's disease (AD), yet the specific pattern of altered connectivity over the course of prodromal AD remains to be characterized. The aim of this study was to assess DMN connectivity in older adults with informant-verified cognitive complaints (CC) but normal neuropsychological performance compared to individuals with mild cognitive impairment (MCI) and healthy controls (HC). DMN maps were derived from resting-state fMRI using independent component analysis. Group comparisons of DMN connectivity were performed between older adults with MCI ($n = 18$), CC ($n = 23$), and HC ($n = 16$). Both CC and MCI showed decreased DMN connectivity in the right hippocampus compared to HC, with the CC group showing greater connectivity than MCI. These differences survived atrophy correction and correlated with cognitive performance. DMN connectivity appears sensitive to early prodromal neurodegenerative changes associated with AD, notably including pre-MCI individuals with cognitive complaints.

Keywords

Alzheimer's disease; cognitive complaints; default mode network; functional connectivity; hippocampus; memory; mild cognitive impairment

INTRODUCTION

The default mode network (DMN) is an interconnected set of brain regions that are spontaneously active when individuals are not focused on the external environment that has been identified using *in vivo* functional neuroimaging techniques [1–4], and consists of a set of brain areas that are tightly functionally connected and distinct from other systems within the brain [2]. Anatomically, the DMN includes: the posterior cingulate cortex (PCC), precuneus, dorsal and ventral medial prefrontal cortex, the lateral (mainly inferior) parietal cortex, and the medial temporal lobes [2–6]. Anatomically distant brain regions within the DMN demonstrate temporal correlations in their spontaneous fluctuations, which represent

© 2013 – IOS Press and the authors. All rights reserved

*Correspondence to: Andrew J. Saykin, PsyD, Center for Neuroimaging, Department of Radiology and Imaging Sciences, Indiana University School of Medicine, 355 W. 16th Street, GH Suite 4100, Indianapolis, IN 46202, USA. Tel.: +1 317 963 7501; Fax: +1 317 963 7547; asaykin@iupui.edu.

Authors' disclosures available online (<http://www.j-alz.com/disclosures/view.php?id=1686>).

functionally coupled intrinsic neuronal processes [2–5, 7]. DMN involves multiple anatomical networks that converge on cortical “hubs”, such as the PCC, ventral medial prefrontal, and inferior parietal cortices. These hubs are strongly inter-connected and show strong connections with the other regions of the DMN [8].

Resting-state functional connectivity magnetic resonance imaging (RS-fcMRI) estimates the coherence in the neural activity across brain regions by measuring patterns of synchronous fluctuations in the blood oxygenation level dependent (BOLD) signal [7] at rest. Emerging evidence suggests that the intrinsic correlations estimated by RS-fcMRI are constrained sufficiently enough by known anatomic connections to be used as a noninvasive probe of the functional connectivity of a neural system [2, 7]. Using advanced RS-fcMRI, the DMN has repeatedly been shown to be altered in AD [6, 8–11]. Greicius and colleagues first noted DMN alterations during the resting state in patients with mild Alzheimer’s disease (AD) compared to age-matched controls, manifesting as decreased functional connectivity between PCC/precuneus and the hippocampus [11]. Subsequently, several groups have reported DMN disruption in mild cognitive impairment (MCI) [9, 12, 13], which is considered to be a prodromal stage of AD, as well as in normal individuals carrying the most significant late-onset AD genetic risk factor, the apolipoprotein E (*APOE*) $\epsilon 4$ allele [14–16], and those with a positive family history of AD [17]. Cognitively normal older adults with significant cortical amyloid deposition have also been shown to have disrupted DMN connectivity [8, 18–20]. Interestingly, two brain areas most prone to significant amyloid deposition, the medial prefrontal cortex and PCC, are also both components of the DMN [8, 18–20]. Other studies have shown that age-related changes in DMN connectivity were found to be more advanced in an AD sample than in normal older adults [21], and that changes in DMN connectivity occur even before significant brain atrophy in patients with AD [11]. Differences in DMN connectivity between stable and progressive MCI were also observed [12]. More interestingly, Damoiseaux and colleagues have evaluated three subnetworks of DMN and found decreased connectivity in the posterior DMN, and increased connectivity in the anterior and ventral DMN at baseline in AD patients versus controls [10]. However, the complete trajectory of changes in DMN connectivity over the course of the preclinical and prodromal stages of AD remains to be elucidated [2, 6].

Previous studies have indicated that older adults with subjective memory impairment have a higher risk for future dementia [22] as well as decreased entorhinal cortex volume [23] and glucose metabolism [24] and therefore as a group may represent a prodromal phase of AD preceding MCI (“pre-MCI”). In euthymic older adults with informant-verified cognitive complaints largely involving memory, our group reported reductions in medial temporal regional grey matter density and alterations in white matter integrity similar in pattern to those seen in MCI and AD [25–28], as well as altered visual contrast sensitivity [29], lending further support to the concept that this group may represent a pre-MCI stage for many individuals.

The goal of the present study was to measure resting-state DMN connectivity in cognitively normal older adults (HC), subjects with informant-verified cognitive complaints (CC; as a pre-MCI group), and MCI patients. We hypothesized that the CC group would show intermediate changes in resting-state DMN connectivity relative to the MCI and HC groups. We also hypothesized that subjective and objective measures of memory integrity would be directly related to DMN connectivity.

MATERIALS AND METHODS

Participants

The study was approved by the Indiana University Institutional Review Board, and written informed consent was obtained from all participants. Participants were consecutively selected on the basis of resting state scan availability from a larger cohort of older adults recruited for a longitudinal study of brain aging and memory. The sample included 23 euthymic individuals with significant cognitive complaints despite cognitive test performance within the normal range (CC group), 18 patients with amnesic MCI (MCI group), and 16 healthy age-matched healthy controls (HC group) without significant cognitive complaints or psychometric deficits. Further details regarding participant recruitment, selection criteria, and characterization are described in Saykin et al. [25] although the present study represents an independent sample.

Inclusion criteria were: at least 60 years of age, right-handed, fluent in English, and at least 10 years of formal education. Participants were required to have an informant who knew them well and could answer questions about their cognition and general health. Exclusion criteria included any significant or uncontrolled medical, psychiatric, or neurologic condition (other than MCI) that could significantly affect brain structure or cognition including but not limited to history of head trauma with loss of consciousness lasting more than 5 minutes, history of substance dependence, and factors contraindicating MRI. Non-amnesic forms of MCI [30] were excluded, although amnesic MCI with involvement of multiple domains was permitted.

Neuropsychological assessment

Participants underwent a detailed neuropsychological evaluation, including measures of memory, attention, executive function, language, spatial ability, general intellectual ability, and psychomotor speed, as well as standard dementia screens. Tests examined for the current analyses included the Mini-Mental State Examination (MMSE) [31], Mattis Dementia Rating Scale-2 [32], and California Verbal Learning Test-II (CVLT-II) [33]. For the CVLT-II, participants were randomly administered either the standard or alternate test forms to reduce practice effects engendered by multiple administrations of the same items. Multiple inventories were employed to assess subjective cognitive functioning, including the Memory Self-Rating Questionnaire [34], self and informant versions of the Neurobehavioral Function and Activities of Daily Living Rating Scale [35], self and informant versions of the Informant Questionnaire on Cognitive Decline in the Elderly [36], the four cognitive items from the Geriatric Depression Scale (GDS) [37], and 23 items from the Memory Assessment Questionnaire [38]. A Cognitive Complaint Index (CCI) was calculated as the percentage of all complaint items positively endorsed [25].

Group classifications (HC, CC, MCI) were based on results of the neuropsychological assessment and self and informant report indices. A multidisciplinary clinical consensus panel reviewed each case according to specific criteria [25]. MCI (amnesic type) subjects had a Clinical Dementia Rating (CDR) global score of 0.5, with 0.5 or greater rating on the memory domain. Participants were categorized as CC if they endorsed more than 20% of the items on the CCI based on our previous work [25] or by consensus appraisal that cognitive concerns were of potential clinical significance.

MR imaging

Imaging data were acquired on a Siemens Tim Trio 3.0 T whole body scanner. Participants were scanned at rest with eyes closed, using a 2D axial T2*-weighted single shot echo planar imaging (EPI) pulse sequence (TR/TE: 2250 ms/29 ms, Flip angle: 79, FOV: 220

mm, Matrix: 88×88, 39 axial slices, voxel size: $2.5 \times 2.5 \times 3.5 \text{ mm}^3$, total 161 measurements). An integrated Parallel Acquisition Techniques (iPAT) accelerator factor of 2 was used to reduce susceptibility artifact. The 3D prospective motion correction algorithm (PACE) was performed during the EPI scan to minimize head motion artifact. In addition, T1-weighted anatomical scans were performed using the Alzheimer's Disease Neuroimaging Initiative (ADNI) Magnetization Prepared Rapid Gradient Echo (MPRAGE) protocol (60 contiguous 1.2 mm sagittal slices, TR/TE: 2300 ms/2.91 ms, Magn. Preparation: Non-sel. IR, TI: 900 ms, Flip angle: 9, in-plane resolution: $1.0 \times 1.0 \text{ mm}^2$, BW: 240 Hz/Px). To detect incidental findings including cerebrovascular abnormalities, a high-resolution (isotropic voxel size of 1 mm^3), 3D Fluid Attenuated Inversion Recovery (FLAIR) sequence was utilized using the following parameters: TR/TE/TI = 5000/361/1800 ms, Flip angle = 180.

Imaging data processing

MPRAGE images were processed using SPM8 (<http://www.fil.ion.ucl.ac.uk/spm/>) according to updated versions of processing procedures described in our prior work [25]. Briefly, the MPRAGE image for each participant was segmented into gray matter (GM), white matter (WM), and cerebrospinal fluid (CSF) compartments. An individual GM density map was also generated for each participant [25]. These GM density maps and volume information were used for further analyses (see below).

To determine degree of brain atrophy, voxel-based morphometry (VBM) was also performed in SPM8 using updated versions of processing procedures as described in our previous publications [25, 39, 40] which include advanced registration and segmentation. In addition, each participant's cortical and subcortical tissue volumes, as well as the total intracranial volume, were estimated using automated parcellation as implemented in the FreeSurfer software package (version 5.1) [41] using the T1-weighted MPRAGE anatomical images [40].

RS-fcMRI data was preprocessed using approaches described by Biswal et al. [7]. All resting-state scans were preprocessed using both AFNI (<http://afni.nimh.nih.gov>) and FSL (<http://www.fmrib.ox.ac.uk>). After the first three images of every scan were discarded to remove possible T1 stabilization effects, images underwent slice-time correction by means of sinc interpolation, followed by motion correction by aligning each volume to the mean image volume using Fourier interpolation. Time series were temporally filtered using a band-pass filter (0.01~0.1 Hz) [7, 13, 14, 17, 20] and processed with linear detrending to remove any residual drift. Image data were then spatially smoothed using a 5-mm FWHM Gaussian kernel. After co-registration to the corresponding MPRAGE image, all EPI data were transformed into the Montréal Neurological Institute (MNI) standard space as 2 mm isotropic voxels. Finally, to control for the effects of physiological processes such as fluctuations related to motion and cardiac and respiratory cycles, nuisance signals were removed from the data via multiple regression. Specifically, each individual's 4D time series data was regressed on nine predictors: white matter, cerebrospinal fluid, the global signal, and six motion parameters [7, 8, 19].

Independent component analysis

All preprocessed individual 4D RS-fcMRI data were temporally concatenated. Independent component analysis (ICA) was then performed on this group data to generate group-level components for the whole sample using the MELODIC function of the FSL package [42]. Consistent with recent work using an ICA approach in RS-fcMRI analysis, the number of components was fixed at 20 [7, 12, 21]. The group ICA was repeated several times using unique randomly resampled data to ensure stability of 20 independent components [7, 21]. A

meta-ICA analysis was then carried out using all iterations of the group ICA components to extract the 20 spatially independent components consistently identified across the group ICA runs. To reconstruct component maps for each participant, dual regression [7, 9, 10, 14, 15, 21] was applied to each individual's preprocessed datasets using the 20 group components identified using the ICA approach as templates. Specifically, for each of the group component templates, the first regression model used the template as a spatial predictor for the participant's 4D data, producing a set of individual regression weights in the time domain. Using this time series as a temporal predictor for the 4D BOLD data, the second regression equation estimated the individual regression weights in the spatial domain. In this work, individual DMN component maps were selected to carry out group-level statistics [7, 9, 10, 14, 15, 21].

Statistical analysis

Voxel level group statistical analyses were carried out using SPM8 on individual DMN maps. The unified statistical model is an ANCOVA, treating diagnostic group (HC, CC, MCI) as the between group factor. F-contrasts were used to measure the effect of diagnostic group, with age and gender as confounding covariates. To take account of the potential effect of underlying GM atrophy, individual GM density maps were added as a voxel-dependent covariate using the Biological Parametric Mapping toolbox [21, 43, 44].

Voxel-wise linear regression was implemented in SPM8 to evaluate the relationship between DMN connectivity and clinical dementia severity (CDR Sum of Boxes (CDR-SB) score), as well as DMN connectivity and memory performance (CVLT-II total score, short delay recall score (CVLT-SD), and long delay recall score (CVLT-LD)). Age at scan, years of education, and gender were included as covariates. Results were masked using a standard whole-brain mask. A voxel-wise threshold of $p < 0.005$ was considered significant for all statistical models.

Statistical Package for Social Sciences (SPSS, version 19.0) was used to assess differences between diagnostic groups in demographic, cognitive variables, and region of interest (ROI) data. For continuous variables, ANOVAs were employed with a Tukey's *post-hoc* test for multiple comparisons, while χ^2 tests were used to assess categorical variables.

RESULTS

Participant characteristics

The three groups of participants did not differ significantly with respect to age or years of education (Table 1). However, in view of slight differences in age and years of education, these variables were entered as covariates in all voxel-wise statistical analyses. Male to female ratio among the three groups was not significantly different by χ^2 test. Assessment of cognitive performance was based on score adjusted for age, years of education, and gender, as applicable [25]. As expected, CC and MCI participants had significantly higher CDR global and sum of boxes scores than HC, whereas no significant differences between CC and MCI groups were found (Table 1). The CCI was significantly elevated in both the CC and MCI groups relative to the HC group. The CC and MCI groups did not differ and endorsed approximately three times as many complaints as the HC group. MCI patients had modestly but significantly lower mean MMSE and DRS-2 total scores than the CC and HC groups. The most significant difference between MCI patients and other participants was observed for the CVLT-II scores (total, short delay, long delay). The CC group was not significantly different from the HC group on the MMSE, DRS-2, and CVLT-II scores. No significant difference in *APOE* $\epsilon 4$ carrier status was observed across the groups although the present study was notably not powered to detect genetic influences.

Group difference in DMN

As predicted, ICA analysis revealed a sample-specific DMN with both anterior and posterior regions present (Fig. 1). At the threshold of $p < 0.005$ (*uncorrected*), voxel-wise between-group analyses (Fig. 2, Table 2), the CC group showed more DMN connectivity in right hippocampus and right precuneus than the MCI group, but demonstrated significantly less DMN connectivity in the right hippocampus compared to the HC group, while significant reduction of DMN connectivity was evident in the MCI group relative to the HC group in the right hippocampus, right parahippocampal gyrus, right precuneus, and right thalamus.

In subsequent ROI analyses, mean Z-score of the DMN component for each participant was extracted from the right hippocampal cluster showing significant voxel-wise differences between HC and MCI groups. Using age, years of education, and gender as covariates, ANOVA indicated a significant difference between groups ($F(2,57) = 9.893, p < 0.005$). *Post-hoc* comparisons showed significant differences between all groups, with HC > MCI ($p < 0.0001$), HC > CC ($p < 0.005$), and CC > MCI ($p < 0.02$) (Fig. 3).

Relationship between memory performance and DMN

At the threshold of $p < 0.005$ (*uncorrected*), a voxel-wise regression analysis yielded clusters showing significant positive associations between CVLT performance and DMN connectivity across the whole sample (Fig. 4). Specifically, positive correlations between DMN connectivity and CVLT-II total score were most evident in the right hippocampus, right hippocampal gyrus, and right thalamus. Likewise, CVLT-II SD and CVLT-II LD scores were also positively correlated with DMN connectivity in the right hippocampus, right hippocampal gyrus, and right thalamus.

Using the right hippocampal cluster showing significant voxel-wise difference in DMN between HC and MCI groups as an ROI, partial correlations controlling for age, years of education, and gender were performed to investigate relationships between right hippocampal DMN connectivity and cognitive indices. Significant negative correlations were observed between the mean right hippocampal ROI DMN Z-score and the CDR global score ($r = -0.45, p < 0.001$), as well as the CDR-SB ($r = -0.38, p < 0.01$). Significant positive correlations were shown between the mean right hippocampal DMN Z-score and CVLT-II performance (CVLT-II total score: $r = 0.53, p < 0.0001$; CVLT-II SD score: $r = 0.53, p < 0.0001$; CVLT-II LD score: $r = 0.51, p < 0.0005$).

Gray matter atrophy

Using age, gender, years of education, and total intracranial volume as covariates, both a VBM voxel-wise analysis and an ANOVA of FreeSurfer-derived cortical and subcortical volumes found no significant difference between groups in GM atrophy along the main components of DMN, including the PCC, precuneus, medial prefrontal cortex, inferior parietal cortex, and medial temporal lobes (bilateral hippocampi).

DISCUSSION

In the present study, the MCI group demonstrated lower connectivity relative to HC and CC groups in key DMN regions, including right hippocampus, precuneus, and right thalamus. These findings are generally in accord with previous DMN studies in MCI and AD [8–15, 18, 21]. The novel aspect of the present report was the inclusion of a group of individuals with marked cognitive complaints but psychometric performance within normal limits. Consistent with study hypotheses, the CC group demonstrated intermediate changes of DMN connectivity in right hippocampus, with values falling between those of the MCI and HC groups. Further, alterations in hippocampal DMN connectivity were significantly

associated with performance on measures of episodic memory and clinical dementia severity.

Volume loss or atrophy of the hippocampus can be observed as one of the earliest and ultimately most significant signs in both MCI and AD, and can also longitudinally predict conversion from MCI to AD over time [39, 40]. In our previous report [25], intermediate decrease in hippocampal volume was observed in participants with CC compared with HC and MCI groups. Structural GM differences between groups were not statistically significant in the current study, likely due to relative small sample size. However, it is also possible that a decrease in functional connectivity within the DMN may precede GM atrophy in the early stages of AD [5, 45]. In other words, our findings could indicate functional changes in the DMN that may precede significant brain atrophy in participants likely to progress to AD. These results suggest that RS-fcMRI can contribute new information related to functional changes at pre-MCI stages of probable AD.

In this study, thalamic connections also demonstrated significant correlations with CVLT-II performance, as well as group differences between HC and MCI. The thalamus is not typically included in DMN but has been shown to play an intermediary role in cortico-cortical interactions [3]. Thalamic abnormalities, including local lesion or reduction of connections, have been associated with disruption in DMN [44, 46]. A recent study showed that thalamic lesions may result in reduced activity in these regions [46], since the PCC receives axonal projections from the anterior thalamic nuclei [47]. This notion is also in line with our previous report showing significant callosal atrophy and in CC and MCI patients relative to healthy controls [27].

The leading hypothesis regarding the causes of AD proposes that toxic forms of the amyloid- β protein initiate a cascade of events ending in synaptic dysfunction and cell death [48]. The pathophysiological process of AD is associated with alterations in large-scale functional brain networks, in particular, the distributed networks supporting memory function [49]. The DMN offers a functional glimpse into regions of particular interest [2, 5, 6, 49]. From the disease prospective, many DMN regions are particularly vulnerable to neuropathologic cellular [50] and structural change in MCI and AD [2, 5, 6, 49]. Specific regions of the DMN, particularly the precuneus and PCC, are selectively vulnerable to early amyloid deposition in AD [8, 18–20]. Recent studies have also revealed that disruption of the intrinsic connectivity of these networks is observable during the resting state even in asymptomatic individuals with high amyloid burden [18–20].

While the nature of DMN function remains elusive, numerous studies of DMN connectivity have been published, likely because it is an easily produced, readily identified, and consistent pattern of brain activity [6]. Activity in DMN regions can be efficiently elicited during simple resting-state scans, a benefit in the study of individuals with compromised health or cognitive ability. Our study provides support for the notion that one of the functions of the DMN is to subservise episodic memory processes [2, 6, 49]. Research is ongoing to determine if impaired connectivity within DMN may serve as a predictor of memory decline related to the development of AD in prodromal stages. Our results, together with other recent findings, suggest that DMN connectivity may be able to serve as an additional stage-related biomarker that can contribute information above and beyond established medial temporal atrophy and cognitive measures. Furthermore, the CC group may represent a pre-MCI stage and may provide an earlier therapeutic opportunity than MCI [22–28].

Acknowledgments

Study funding supported in part by grants from National Institutes of Health, NIA R01 AG19771 and Indiana Economic Development Corporation, IEDC #87884 (to AJS); National Institutes of Health, NIA P30 AG10133-18S1 Core Supplement to Drs. B. Ghetti and AJS.

References

1. Raichle ME, MacLeod AM, Snyder AZ, Powers WJ, Gusnard DA, Shulman GL. A default mode of brain function. *Proc Natl Acad Sci U S A*. 2001; 98:676–682. [PubMed: 11209064]
2. Buckner RL, Andrews-Hanna JR, Schacter DL. The brain's default network: Anatomy, function, and relevance to disease. *Ann N Y Acad Sci*. 2008; 1124:1–38. [PubMed: 18400922]
3. Greicius MD, Krasnow B, Reiss AL, Menon V. Functional connectivity in the resting brain: A network analysis of the default mode hypothesis. *Proc Natl Acad Sci U S A*. 2003; 100:253–258. [PubMed: 12506194]
4. Fox MD, Snyder AZ, Vincent JL, Corbetta M, Van Essen DC, Raichle ME. The human brain is intrinsically organized into dynamic, anticorrelated functional networks. *Proc Natl Acad Sci U S A*. 2005; 102:9673–9678. [PubMed: 15976020]
5. Mevel K, Chetelat G, Eustache F, Desgranges B. The default mode network in healthy aging and Alzheimer's disease. *Int J Alzheimers Dis*. 2011; 2011:535816. [PubMed: 21760988]
6. Beason-Held LL. Dementia and the default mode. *Curr Alzheimer Res*. 2011; 8:361–365. [PubMed: 21222595]
7. Biswal BB, Mennes M, Zuo XN, Gohel S, Kelly C, Smith SM, Beckmann CF, Adelstein JS, Buckner RL, Colcombe S, Dogonowski AM, Ernst M, Fair D, Hampson M, Hoptman MJ, Hyde JS, Kiviniemi VJ, Kotter R, Li SJ, Lin CP, Lowe MJ, Mackay C, Madden DJ, Madsen KH, Margulies DS, Mayberg HS, McMahon K, Monk CS, Mostofsky SH, Nagel BJ, Pekar JJ, Peltier SJ, Petersen SE, Riedl V, Rombouts SA, Rypma B, Schlaggar BL, Schmidt S, Seidler RD, Siegle GJ, Sorg C, Teng GJ, Veijola J, Villringer A, Walter M, Wang L, Weng XC, Whitfield-Gabrieli S, Williamson P, Windischberger C, Zang YF, Zhang HY, Castellanos FX, Milham MP. Toward discovery science of human brain function. *Proc Natl Acad Sci U S A*. 2010; 107:4734–4739. [PubMed: 20176931]
8. Buckner RL, Sepulcre J, Talukdar T, Krienen FM, Liu H, Hedden T, Andrews-Hanna JR, Sperling RA, Johnson KA. Cortical hubs revealed by intrinsic functional connectivity: Mapping, assessment of stability, and relation to Alzheimer's disease. *J Neurosci*. 2009; 29:1860–1873. [PubMed: 19211893]
9. Binnewijzend MA, Schoonheim MM, Sanz-Arigita E, Wink AM, van der Flier WM, Tolboom N, Adriaanse SM, Damoiseaux JS, Scheltens P, van Berckel BN, Barkhof F. Resting-state fMRI changes in Alzheimer's disease and mild cognitive impairment. *Neurobiol Aging*. 2012; 33:2018–2028. [PubMed: 21862179]
10. Damoiseaux JS, Prater KE, Miller BL, Greicius MD. Functional connectivity tracks clinical deterioration in Alzheimer's disease. *Neurobiol Aging*. 2012; 33:828, e819–e830. [PubMed: 21840627]
11. Greicius MD, Srivastava G, Reiss AL, Menon V. Default-mode network activity distinguishes Alzheimer's disease from healthy aging: Evidence from functional MRI. *Proc Natl Acad Sci U S A*. 2004; 101:4637–4642. [PubMed: 15070770]
12. Petrella JR, Sheldon FC, Prince SE, Calhoun VD, Doraiswamy PM. Default mode network connectivity in stable vs progressive mild cognitive impairment. *Neurology*. 2011; 76:511–517. [PubMed: 21228297]
13. Sorg C, Riedl V, Muhlau M, Calhoun VD, Eichele T, Laer L, Drzezga A, Forstl H, Kurz A, Zimmer C, Wohlschlagger AM. Selective changes of resting-state networks in individuals at risk for Alzheimer's disease. *Proc Natl Acad Sci U S A*. 2007; 104:18760–18765. [PubMed: 18003904]
14. Filippini N, MacIntosh BJ, Hough MG, Goodwin GM, Frisoni GB, Smith SM, Matthews PM, Beckmann CF, Mackay CE. Distinct patterns of brain activity in young carriers of the APOE-epsilon4 allele. *Proc Natl Acad Sci U S A*. 2009; 106:7209–7214. [PubMed: 19357304]

15. Westlye ET, Lundervold A, Rootwelt H, Lundervold AJ, Westlye LT. Increased hippocampal default mode synchronization during rest in middle-aged and elderly APOE epsilon4 carriers: Relationships with memory performance. *J Neurosci*. 2011; 31:7775–7783. [PubMed: 21613490]
16. Patel KT, Stevens MC, Pearlson GD, Winkler AM, Hawkins KA, Skudlarski P, Bauer LO. Default mode network activity and white matter integrity in healthy middle-aged ApoE4 carriers. *Brain Imaging Behav*. 2013; 7:60–67. [PubMed: 23011382]
17. Fleisher AS, Sherzai A, Taylor C, Langbaum JB, Chen K, Buxton RB. Resting-state BOLD networks versus task-associated functional MRI for distinguishing Alzheimer's disease risk groups. *Neuroimage*. 2009; 47:1678–1690. [PubMed: 19539034]
18. Sperling RA, Laviolette PS, O'Keefe K, O'Brien J, Rentz DM, Pihlajamaki M, Marshall G, Hyman BT, Selkoe DJ, Hedden T, Buckner RL, Becker JA, Johnson KA. Amyloid deposition is associated with impaired default network function in older persons without dementia. *Neuron*. 2009; 63:178–188. [PubMed: 19640477]
19. Drzezga A, Becker JA, Van Dijk KR, Sreenivasan A, Talukdar T, Sullivan C, Schultz AP, Sepulcre J, Putcha D, Greve D, Johnson KA, Sperling RA. Neuronal dysfunction and disconnection of cortical hubs in non-demented subjects with elevated amyloid burden. *Brain*. 2011; 134:1635–1646. [PubMed: 21490054]
20. Mormino EC, Smiljic A, Hayenga AO, Onami SH, Greicius MD, Rabinovici GD, Janabi M, Baker SL, Yen IV, Madison CM, Miller BL, Jagust WJ. Relationships between beta-amyloid and functional connectivity in different components of the default mode network in aging. *Cereb Cortex*. 2011; 21:2399–2407. [PubMed: 21383234]
21. Jones DT, Machulda MM, Vemuri P, McDade EM, Zeng G, Senjem ML, Gunter JL, Przybelski SA, Avula RT, Knopman DS, Boeve BF, Petersen RC, Jack CR Jr. Age-related changes in the default mode network are more advanced in Alzheimer disease. *Neurology*. 2011; 77:1524–1531. [PubMed: 21975202]
22. Jessen F, Wiese B, Bachmann C, Eifflaender-Gorfer S, Haller F, Kolsch H, Luck T, Mosch E, van den Bussche H, Wagner M, Wollny A, Zimmermann T, Pentzek M, Riedel-Heller SG, Romberg HP, Weyerer S, Kaduszkiewicz H, Maier W, Bickel H. Prediction of dementia by subjective memory impairment: Effects of severity and temporal association with cognitive impairment. *Arch Gen Psychiatry*. 2010; 67:414–422. [PubMed: 20368517]
23. Jessen F, Feyen L, Freymann K, Tepest R, Maier W, Heun R, Schild HH, Scheef L. Volume reduction of the entorhinal cortex in subjective memory impairment. *Neurobiol Aging*. 2006; 27:1751–1756. [PubMed: 16309795]
24. Scheef L, Spottke A, Daerr M, Joe A, Striepens N, Kolsch H, Popp J, Daamen M, Gorris D, Heneka MT, Boecker H, Biersack HJ, Maier W, Schild HH, Wagner M, Jessen F. Glucose metabolism, gray matter structure, and memory decline in subjective memory impairment. *Neurology*. 2012; 79:1332–1339. [PubMed: 22914828]
25. Saykin AJ, Wishart HA, Rabin LA, Santulli RB, Flashman LA, West JD, McHugh TL, Mamourian AC. Older adults with cognitive complaints show brain atrophy similar to that of amnesic MCI. *Neurology*. 2006; 67:834–842. [PubMed: 16966547]
26. Wang Y, West JD, Flashman LA, Wishart HA, Santulli RB, Rabin LA, Pare N, Arfanakis K, Saykin AJ. Selective changes in white matter integrity in MCI and older adults with cognitive complaints. *Biochim Biophys Acta*. 2012; 1822:423–430. [PubMed: 21867750]
27. Wang PJ, Saykin AJ, Flashman LA, Wishart HA, Rabin LA, Santulli RB, McHugh TL, MacDonald JW, Mamourian AC. Regionally specific atrophy of the corpus callosum in AD, MCI and cognitive complaints. *Neurobiol Aging*. 2006; 27:1613–1617. [PubMed: 16271806]
28. Copenhaver BR, Rabin LA, Saykin AJ, Roth RM, Wishart HA, Flashman LA, Santulli RB, McHugh TL, Mamourian AC. The fornix and mammillary bodies in older adults with Alzheimer's disease, mild cognitive impairment, and cognitive complaints: A volumetric MRI study. *Psychiatry Res*. 2006; 147:93–103. [PubMed: 16920336]
29. Risacher SL, Wudunn D, Pepin SM, Magee TR, McDonald BC, Flashman LA, Wishart HA, Pixley HS, Rabin LA, Pare N, Englert JJ, Schwartz E, Curtain JR, West JD, O'Neill DP, Santulli RB, Newman RW, Saykin AJ. Visual contrast sensitivity in Alzheimer's disease, mild cognitive impairment, and older adults with cognitive complaints. *Neurobiol Aging*. 2013; 34:1133–1144. [PubMed: 23084085]

30. Petersen RC. Mild cognitive impairment as a diagnostic entity. *J Intern Med.* 2004; 256:183–194. [PubMed: 15324362]
31. Folstein MF, Folstein SE, McHugh PR. “Mini Mental State”: A practical method for grading the cognitive state of patients for the clinician. *J Psychiatry Res.* 1975; 12:189–198.
32. Jurica, P.; Leitten, C.; Mattis, S. *Dementia Rating Scale-2.* Psychological Assessment Resources, Inc; Lutz, FL: 2001.
33. Delis, DC.; Kramer, JH.; Kaplan, E.; Ober, BA. *California Verbal Learning Test-Second Edition: Adult Version Manual.* The Psychological Corporation; San Antonio, TX: 2000.
34. Squire LR, Wetzel CD, Slater PC. Memory complaint after electroconvulsive therapy: Assessment with a new self-rating instrument. *Biol Psychiatry.* 1979; 14:791–801. [PubMed: 497304]
35. Saykin, AJ. *Neurobehavioral function and activities of daily living rating scale (NBFADL-63 item version).* Dart-mouth Medical School; Hanover: 1992.
36. Jorm AF, Jacomb PA. An informant questionnaire on cognitive decline in the elderly (IQCODE): Socio-demographic correlates reliability, validity and some norms. *Psychol Med.* 1989; 19:1015–1022. [PubMed: 2594878]
37. Yesavage JA, Brink TL, Lose TL, Lum O, Huang V, Adey M, Leirer VO. Development and validation of geriatric depression rating scale: A preliminary report. *J Psychiat Res.* 1982; 17:37–49. [PubMed: 7183759]
38. Santulli, R.; Saykin, A.; Rabin, L.; Wishart, H.; Flashman, L.; Pare, N.; Nutter-Upham, K.; Pixley, H. Differential sensitivity of cognitive complaints associated with amnesic MCI: Analysis of patient and informant reports. *Alzheimer’s Association International Conference on the Prevention of Dementia;* Washington, DC. 2005.
39. Risacher SL, Saykin AJ, West JD, Shen L, Firpi HA, McDonald BC. Baseline MRI predictors of conversion from MCI to probable AD in the ADNI cohort. *Curr Alzheimer Res.* 2009; 6:347–361. [PubMed: 19689234]
40. Risacher SL, Shen L, West JD, Kim S, McDonald BC, Beckett LA, Harvey DJ, Jack CR Jr, Weiner MW, Saykin AJ. Longitudinal MRI atrophy biomarkers: Relationship to conversion in the ADNI cohort. *Neurobiol Aging.* 2010; 31:1401–1418. [PubMed: 20620664]
41. Fischl B, Salat DH, Busa E, Albert M, Dieterich M, Haselgrove C, van der Kouwe A, Killiany R, Kennedy D, Klaveness S, Montillo A, Makris N, Rosen B, Dale AM. Whole brain segmentation: Automated labeling of neuroanatomical structures in the human brain. *Neuron.* 2002; 33:341–355. [PubMed: 11832223]
42. Beckmann CF, DeLuca M, Devlin JT, Smith SM. Investigations into resting-state connectivity using independent component analysis. *Philos Trans R Soc Lond B Biol Sci.* 2005; 360:1001–1013. [PubMed: 16087444]
43. Casanova R, Srikanth R, Baer A, Laurienti PJ, Burdette JH, Hayasaka S, Flowers L, Wood F, Maldjian JA. Biological parametric mapping: A statistical toolbox for multimodality brain image analysis. *Neuroimage.* 2007; 34:137–143. [PubMed: 17070709]
44. Zhou J, Greicius MD, Gennatas ED, Growdon ME, Jang JY, Rabinovici GD, Kramer JH, Weiner M, Miller BL, Seeley WW. Divergent network connectivity changes in behavioural variant frontotemporal dementia and Alzheimer’s disease. *Brain.* 2010; 133:1352–1367. [PubMed: 20410145]
45. Gili T, Cercignani M, Serra L, Perri R, Giove F, Maraviglia B, Caltagirone C, Bozzali M. Regional brain atrophy and functional disconnection across Alzheimer’s disease evolution. *J Neurol Neurosurg Psychiatry.* 2011; 82:58–66. [PubMed: 20639384]
46. Jones DT, Mateen FJ, Lucchinetti CF, Jack CR Jr, Welker KM. Default mode network disruption secondary to a lesion in the anterior thalamus. *Arch Neurol.* 2011; 68:242–247. [PubMed: 20937938]
47. Vogt BA, Laureys S. Posterior cingulate, precuneal and retrosplenial cortices: Cytology and components of the neural network correlates of consciousness. *Prog Brain Res.* 2005; 150:205–217. [PubMed: 16186025]
48. Jack CR Jr, Knopman DS, Jagust WJ, Shaw LM, Aisen PS, Weiner MW, Petersen RC, Trojanowski JQ. Hypothetical model of dynamic biomarkers of the Alzheimer’s pathological cascade. *Lancet Neurol.* 2010; 9:119–128. [PubMed: 20083042]

49. Sperling RA, Dickerson BC, Pihlajamaki M, Vannini P, LaViolette PS, Vitolo OV, Hedden T, Becker JA, Rentz DM, Selkoe DJ, Johnson KA. Functional alterations in memory networks in early Alzheimer's disease. *Neuromolecular Med.* 2010; 12:27–43. [PubMed: 20069392]
50. Morris JC, Price JL. Pathologic correlates of nondemented aging, mild cognitive impairment, and early-stage Alzheimer's disease. *J Mol Neurosci.* 2001; 17:101–118. [PubMed: 11816784]

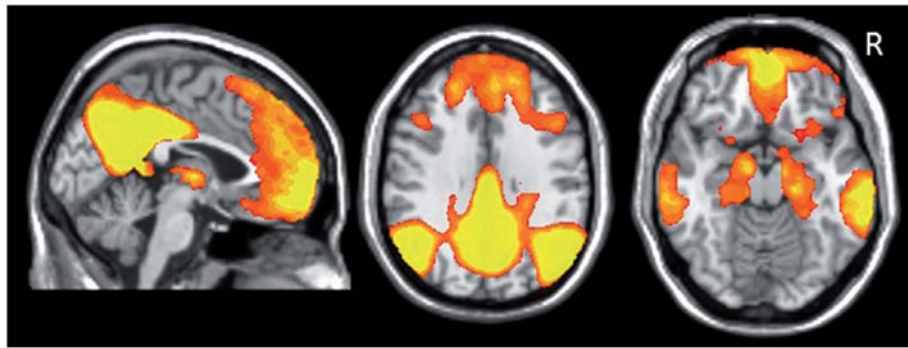


Fig. 1. Illustration of default model network (DMN) regions derived from group independent component analysis (ICA). The DMN component identified by meta-ICA analysis included the posterior cingulate cortex, precuneus, medial prefrontal cortex, lateral parietal regions, lateral temporal regions, and bilateral medial temporal regions ($p < 10^{-4}$).

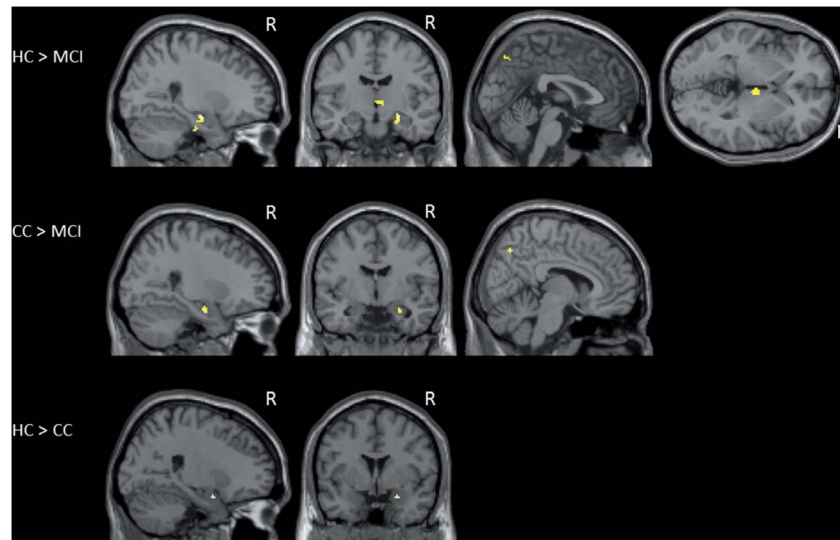


Fig. 2. Brain regions displaying significant differences in default model network connectivity between diagnostic groups (HC, CC, MCI) using voxel-wise comparisons ($p < 0.005$, uncorrected for multiple comparisons). Individual atrophy was controlled using biological parametric mapping.

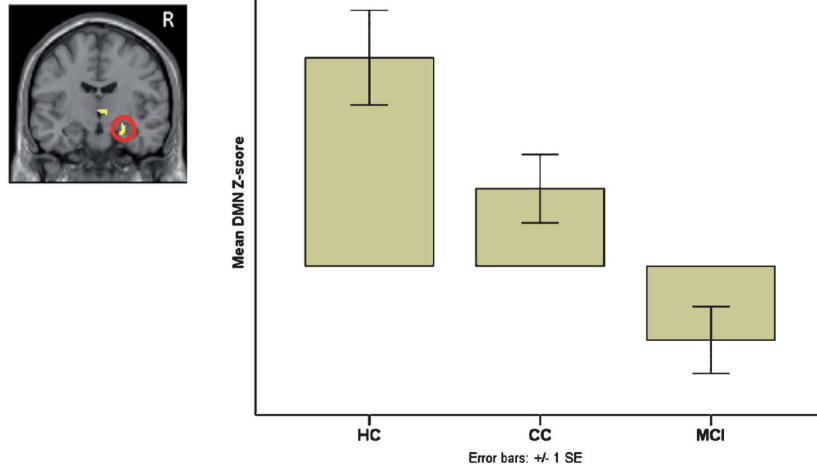


Fig. 3. Region of interest analysis of default mode network (DMN) connectivity in the right hippocampus showed significant differences in DMN Z-scores (\pm SE) between groups (HC > CC > MCI; $p < 0.02$), covaried for age, years of education, and gender.

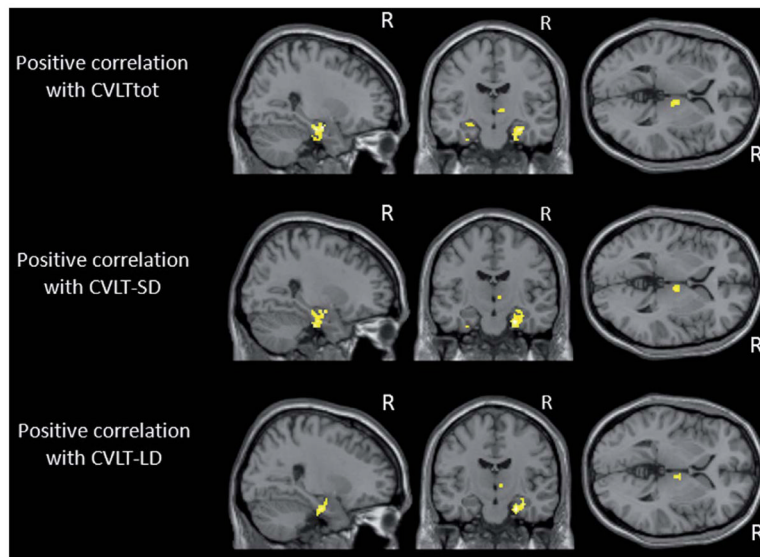


Fig. 4. Verbal memory performance was positively associated with default mode network connectivity in the right hippocampus, right parahippocampal region, and right thalamus across the entire sample ($n = 57$; $p < 0.005$, covaried for age, years of education, and gender). (CVLTtot, California Verbal Learning Test-II total learning raw score; CVLT-SD, CVLT-II short delay recall score; CVLT-LD, CVLT-II long delay recall score).

Table 1

Sample characteristics (mean ± SD)

	HC (n = 16)	CC (n = 23)	MCI (n = 18)	F/χ^2	p value	Post-hoc comparisons (p < 0.05*)
Age (y)	70.7 (6.0)	70.1 (7.3)	73.7 (9.1)	1.219	0.304	NS
Education (y)	17.5 (1.8)	17.0 (1.8)	15.8 (2.9)	2.838	0.067	NS
Gender (M/F)	4:12	8:15	8:10	1.408	0.495	NS
CDR-GL	0.00 (0.0)	0.48 (0.1)	0.50 (0.0)	309.7	<1 × 10 ⁻²⁹	MCI > HC, CC > HC
CDR-SB	0.09 (0.2)	1.06 (0.56)	1.35 (0.29)	42.64	<1 × 10 ⁻¹¹	MCI > HC, CC > HC
CCI	7.9 (4.6)	21.0 (10.7)	24.7 (16.4)	9.572	<1 × 10 ⁻³	MCI > HC, CC > HC
MMSE	28.9 (0.9)	29.2 (1.0)	27.9 (1.2)	7.203	0.002	HC > MCI, CC > MCI
DRStot	140.9 (2.3)	139.6 (3.0)	135.8 (6.0)	7.265	0.002	HC > MCI, CC > MCI
CVLTtot	55.5 (10.1)	53.5 (8.8)	40.3 (6.8)	16.51	<1 × 10 ⁻⁵	HC > MCI, CC > MCI
CVLT-SD	12.8 (2.3)	12.0 (2.2)	8.7 (2.2)	17.78	<1 × 10 ⁻⁵	HC > MCI, CC > MCI
CVLT-LD	13.4 (2.3)	11.9 (2.5)	9.0 (2.9)	13.14	<1 × 10 ⁻³	HC > MCI, CC > MCI
<i>APOE4</i> (±)	11:5 ¹	16:7	9:9	1.960	0.375	NS

Demographic and cognitive characteristics include mean (standard deviation (SD)) for each group. HC, healthy control; CC, cognitive complaints; MCI, mild cognitive impairment; NS, not significant; CDR, Clinical Dementia Rating Scale; CDR-GL, CDR global score; CDR-SB, CDR sum of boxes score; CCI, Cognitive Complaint Index; MMSE, Mini-Mental State Examination total score (maximum 30); DRStot, Dementia Rating Scale-2 total score (maximum 144); CVLTtot, California Verbal Learning Test-II total learning raw score (maximum 80); CVLT-LD, CVLT-II long delay recall score (maximum 16); CVLT-SD, CVLT-II short delay recall score (maximum 16).

¹Missing *APOE* genotype data for 1 HC participant;

* After correction for multiple comparisons.

Table 2

Brain clusters showing differences in DMN connectivity between groups after controlling for gray matter density ($p < 0.005$, unc)

Contrast	Brain region	Cluster size (mm ³)	T score	P_{unc}	Peak MNI coordinates (mm)		
					x	y	z
HC > MCI	Right hippocampus	424	4.38	<0.001	28	-12	-14
HC > MCI	Right hippocampal Gyrus	224	3.80	<0.001	28	-20	-32
HC > MCI	Right thalamus	176	3.35	0.001	6	-12	0
HC > MCI	Right precuneus	48	2.90	0.003	2	-74	52
CC > MCI	Right hippocampus	112	3.15	0.001	26	-8	-20
CC > MCI	Right precuneus	72	3.21	0.001	8	-68	46
HC > CC	Right hippocampus	56	3.29	0.001	24	2	-20

HC, healthy control; CC, cognitive complaints; MCI, mild cognitive impairment.